Measuring the Interactions between Carbon Black Nanoparticles and Latex Thin Films in Aqueous Media using AFM Force Spectroscopy

Measuring the Interactions between Carbon Black Nanoparticles and Latex Thin Films in Aqueous Media using AFM Force Spectroscopy

Jake McClements*, Mei Zhang, Norbert Radacsi, Vasileios Koutsos*

School of Engineering, Institute for Materials and Processes, The University of Edinburgh, Sanderson Building, King's Buildings, Edinburgh EH9 3FB, United Kingdom

Abstract

AFM force spectroscopy was utilised to measure the interactions between latex and carbon black nanoparticles in neutral ultrapure water and basic ultrapure water with 0.7% ammonia (pH of 11.6 ± 0.05) by weight added. For the first time, carbon black nanoparticles were adhered to AFM tips with epoxy using force spectroscopy techniques and characterised using SEM and AFM. The carbon-functionalised tips were then utilised to interact with thin films (prepared from concentrated and field latex suspensions) in the two liquid media. The results demonstrated that both attractive (during tip approach) and adhesive (during tip retraction) forces were considerably greater between the latex and carbon nanoparticles when the experiments were carried out in ultrapure water compared to ultrapure water with 0.7% ammonia. This was because the basic ammonia solution increased the negative surface charges of the latex and carbon particles which was confirmed by zeta potential measurements. Therefore, in the ammonia solution, only repulsion was observed on the tip approach and only small amounts of adhesion were observed on the tip retraction. Furthermore, the results demonstrated that despite the different processing and treatment of the concentrated and field latex samples, their interactions with the carbon black nanoparticles were similar in each medium. This study directly measures the interactions between carbon black nanoparticles and natural rubber latex, which has a significance for the manufacturing of automotive tyres and other polymer/carbon composites.

Keywords

Atomic Force Microscopy, Force Spectroscopy, Carbon Black Nanoparticles, Latex, Nanocomposites, Thin Films, Intermolecular Interactions, DLVO Theory

Introduction

Understanding the fundamental interactions between different materials at the nanoscale is vitally important for many applications including thin films,[1,2] coatings,[3] adhesives[4] and advanced composite materials.[5] In particular, characterising the interactions between polymers and carbon-based materials at the nanoscale has huge significance within the composite material industry.[6,7] Understanding these interactions can have substantial impacts on improving both the manufacturing processes and overall bulk properties of polymer/carbon (nano)composites.[8]

AFM force spectroscopy is an extremely versatile tool which can characterise the interactions between different materials at the nanoscale.[9,10] In these experiments, AFM probes are usually modified so that their tips are end-terminated with a particular material. Force spectroscopy is then utilised to bring the tip into contact with the desired surface in order to directly measure the interactions between the two materials.[9] There are many different methods employed to end-terminate AFM tips. For example, tips can be coated with thin layers of materials, such as gold and diamond.[11] This method is fairly common and coated tips can be directly purchased from suppliers. Single polymer chains (synthetic and biopolymer) can also be chemically functionalised to AFM tips in order to investigate the forces associated with single-chain adhesion at surfaces.[1,10,12] Micron-sized materials are generally too large to be directly adhered to the end of an AFM tip. Instead, they are attached to tipless AFM cantilevers which effectively creates a tip composed of the desired micron-sized material. This tip preparation method is relatively simple and experiments have been performed using tips composed of a wide array of different materials including silica and carbon spheres,[13–15] cells,[16] bubbles and oil droplets.[17,18]

Force spectroscopy experiments which investigate the interactions between nanoparticles and surfaces are not common, despite these systems having widespread use in industrial applications and processes. The main reason for this is that the methods of adhering nanoparticles to AFM tips are laborious and complex due to their extremely small size.[19] However, a small number of studies have successfully adhered nanoparticles to AFM tips using different techniques. The majority of these investigations use wet chemistry procedures to end-functionalise AFM tips with either gold or silver nanoparticles and measure their interactions with solid surfaces, such as mica.[20–22]

Additionally, a study by Ong and Sokolov attached various ceria nanoparticles to tips with epoxy using AFM methods and measured ceria-silicon interactions.[19] This method proved to be reliable and many tips were successfully functionalised with ceria nanoparticles.

There have been no studies which have adhered carbon black nanoparticles to AFM tips for force spectroscopy experiments. Consequently, the interactions between carbon black nanoparticles and natural rubber latex have never been directly investigated. However, understanding these interactions is of great importance for the manufacturing of rubber automotive tyres, where carbon black nanoparticles are used as a filler component.[23,24] Some materials used in the manufacturing of tyres for heavy goods vehicles are created by mixing carbon black and natural rubber latex in an aqueous medium. Within this process, it is vital that the carbon becomes homogeneously dispersed within the latex to ensure that the tyres have consistent physical properties. Furthermore, understanding the fundamental interactions between polymers and carbon surfaces is also very useful for many other (nano)composite materials which use carbon filler components, such as nanotubes, graphene and fibres.[6,8,25,26] The current investigation has characterised the interactions between two types of natural rubber latex and carbon black nanoparticles in neutral ultrapure water and basic ultrapure water with 0.7% ammonia. It highlights that there can be significant differences in the carbon-latex interactions in each solution, due to the change in pH levels. The results of these experiments can aid in the manufacturing process of automotive tyres and other polymer/carbon composites which can ultimately lead to products with more favourable and consistent properties. Furthermore, the force spectroscopy experiments appear to be the first to use a nanoparticle-functionalised AFM tip to interact with a polymer thin film (in various aqueous media) rather than a homogeneous solid substrate, such as mica or silicon. This advance in experimental methodology opens up a new avenue for different force spectroscopy investigations on a plethora of colloidal systems with significance to industrial applications and processes.

Experimental

Materials: The experiments were carried out with two commonly utilised forms of natural rubber provided by Michelin: field latex and concentrated latex. Both samples

were harvested from the *Hevea brasiliensis* tree and are composed of a colloidal system containing polyisoprene globules, water, proteins, carbohydrates, lipids and inorganic particles.[27,28] The field latex underwent minimal treatment and processing after harvesting and had a dry rubber content of 28%. Whereas, the concentrated latex experienced centrifuging which increased its dry rubber content to 60%. In all the experiments, N234 carbon black nanoparticles (Cabot Corp, Boston, MA, USA) with a primary diameter of 20 nm were used. The AFM force spectroscopy experiments were carried out in ultrapure water (UPW, SG water Ultrapure water system, offering water quality of resistivity 18.2 MΩ-cm and pH 6.998), and ultrapure water with 0.7% ammonia by weight added (0.7% ammonia UPW). The 0.7% ammonia UPW was measured using an ETI 8000 (ETI, West Sussex, UK) and was more basic with a pH of 11.6 ± 0.05.

Thin Film Preparation: The latex thin films were prepared by initially diluting the concentrated latex and field latex samples with UPW. The concentrated latex was diluted to 1:1000, whilst the field latex was diluted to 1:200. By using AFM imaging, these particular concentrations were deemed to be the most appropriate for creating stable latex thin films on the substrates. For the main experiments, 10 μL of the latex solutions were drop cast onto clean borosilicate glass substrates and left in ambient conditions to dry for 16 - 24 hours. The thin films were then characterised in UPW and 0.7% ammonia UPW using AFM imaging.

AFM Tip Preparation: Epoxy was utilised to adhere the carbon black nanoparticles to the AFM tips using a technique adapted from Ong and Sokolov.[19] Araldite Standard 90 minute two-part epoxy (Araldite, Basil, Switzerland) was thoroughly mixed and an extremely small droplet of the epoxy was then spread thinly across a clean glass substrate using a sterile syringe needle. A small amount of carbon black, which was ground using an agate pestle and mortar, was spread across another clean glass substrate. The two glass substrates were then placed side-by-side in a petri dish which was loaded into the stage of an MFP-1D AFM (Asylum Research, Santa Barbara, CA, USA). The AFM was mounted on a Nikon TE2000-U inverted optical microscope (Nikon UK Limited, Surrey, UK) which allowed the epoxy and carbon black to be examined under high magnification. The AFM and microscope were then utilised to position the tip directly above an epoxy droplet with a diameter which was significantly smaller than the height of the tip (8 μm). This ensured that only a small amount of epoxy would be located at the end of the tip, and

would not engulf the whole tip and cantilever. The tip was then brought into contact with the epoxy droplet for 1 second and then retracted from the surface.

After retraction, the epoxy covered tip was left to partially cure for around 10 minutes. The tip was then brought into contact with a small aggregate of carbon black nanoparticles on the adjacent glass substrate for 1 minute. The AFM tip was then placed in an oven at 60°C for 24 hours to ensure the epoxy was completely cured. After removal from the oven, the tips were thoroughly rinsed with UPW in order to remove any carbon black which was not firmly adhered to the tip. Control experiments were carried out using tips which were functionalised with only epoxy. These tips were prepared using identical methods, but they were put into the oven immediately after contact with the epoxy droplet.

AFM Tip Characterisation: Rigorous characterisation was carried out on the functionalised tips in order to confirm that carbon black was firmly adhered to the very end of them. This involved AFM imaging the carbon black aggregates at the end of the tips using a TGT1 inverted grid (NT-MDT, MSK, Russia). The TGT1 inverted grid is composed of silicon spikes and when it is imaged using AFM, it produces a repeating image of the AFM tip. This allowed each tip to be closely examined at the nanoscale to ensure that they were functionalised by carbon black. Figure 1a shows a typical 3D AFM image of a carbon black-functionalised tip and Figure 1b shows the corresponding profile plot of the tip's surface. The profile plot clearly shows that the tip is end-functionalised with a small aggregate of carbon black. SEM imaging using a JEOL JSM-IT100 (JEOL, Tokyo, Japan) was also utilised to image the functionalised tips, although the scanning was carried out only briefly on each tip to minimise any surface degradation. Figure 1c shows a corresponding SEM image of the typical functionalised AFM tip, where carbon black aggregates can clearly be observed at the end of the tip.

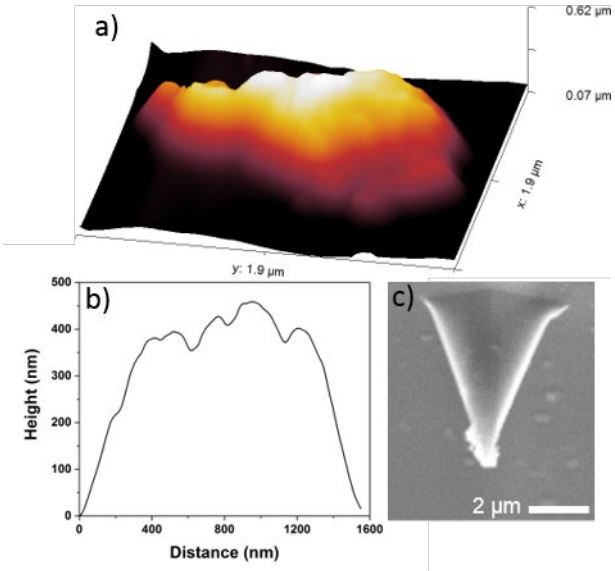

Figure 1: a) Typical 3D image of a carbon black-functionalised AFM tip, produced using a TGT1 grid. b) A corresponding profile plot showing the surface of the functionalised tip. c) A corresponding SEM image of the functionalised tip.

In addition to the TGT1 grid and SEM imaging, a further experiment was also performed to confirm the carbon-latex interactions. This experiment compared the median attractive (minimum force during the approach of the tip) and adhesive force (minimum force during the retraction of the tip) between the field latex and blank tips, epoxy-functionalised tips and carbon black-functionalised tips. The experiments were carried out in UPW using a force setpoint of 0.5 nN (maximum cantilever force exerted), and the results are presented in Figure 2. In the experiment, three different carbon black tips were used to increase the reliability of the results. The graphs in Figure 2 show similar trends and demonstrate that the magnitude of the attraction/adhesion is different for each tip type. This suggests that the tips were end-functionalised with carbon black and that there were no voids or holes where exposed epoxy or the silicon tip could interact with the latex instead. These results, alongside the TGT1 and SEM images, confirm that carbon-latex interactions were successfully measured during the experiments.

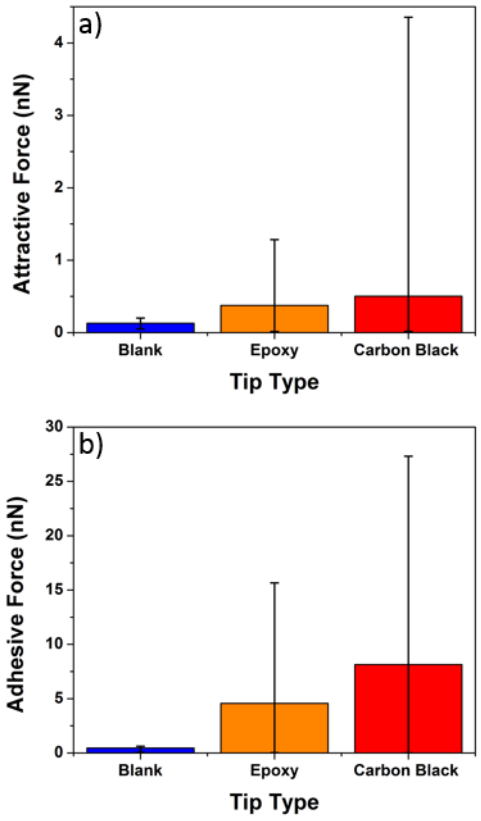

Figure 2: Graphs showing the median attractive and adhesive force between the field latex and blank tips, epoxy-functionalised tips and carbon black-functionalised tips. The experiments were carried out at a setpoint of 0.5 nN in UPW. The bars in the graphs represent the maximum and minimum values within each data set. a) Attractive force, b) adhesive force.

AFM Imaging and Force Spectroscopy: All AFM imaging and force spectroscopy was carried out using a Bruker NanoWizard 4 (Bruker, Santa Barbara, CA, USA) in either UPW or 0.7% ammonia UPW. All imaging was carried out in quantitative imaging (QI) mode using Olympus BL-AC40TS probes with a nominal spring constant of 0.9 N/m. For the force spectroscopy experiments, carbon black-functionalised Bruker MSNL-10 tips with nominal spring constants of 0.01 N/m were used. The force spectroscopy experiments were carried out in UPW and 0.7% ammonia UPW for both the concentrated latex and field latex. Three different carbon black-functionalised tips were used for each experiment (12 in total) which ensured that a large number of force-distance curves (approximately 12,000) were obtained. Each carbon black tip interacted with at least 15

different areas of the latex films and approach/retract cycles were carried out at 5 different force setpoints (0.1 nN, 0.2 nN, 0.5 nN, 1.0 nN and 1.5 nN) at each area. The force setpoint is defined as the maximum force that is applied to the cantilever on the tip approach before retraction begins. Figure 3 shows a typical force-distance curve collected during the force spectroscopy experiments. The graph shows the carbon-concentrated latex interactions on the tip approach and retraction in UPW at a setpoint of 1.5 nN. The annotations highlight the key features on the graph; the initial repulsion on approach, the attractive force on approach, the setpoint force and the adhesive force on retraction.

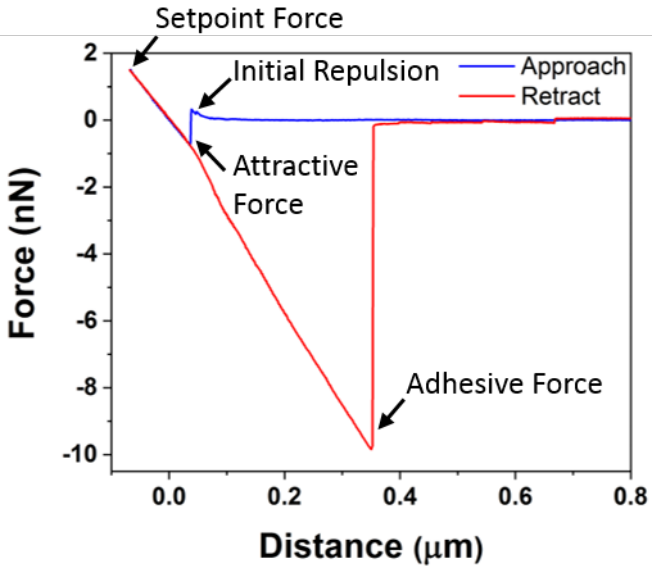

Figure 3: Example of a force-distance curve collected in the force spectroscopy experiments. Annotated labels show the key features of the graph. The graph shows the concentrated latex-carbon interactions in UPW at a setpoint of 1.5 nN.

Zeta-Potential Sample Preparation: To verify the existence of surface charges on the carbon black and latex particles, Zeta potential (ζ-potential) measurements were conducted using a Brookhaven ZetaPALS apparatus. Carbon black was ground with mortar and pestle, then 2.0 mg of powder was distributed into 20 mL of UPW. The mixture was first sonicated at room temperature for 10 min to form a black suspension. 1 mL of the as-prepared suspension was further diluted in 9 mL UPW and further sonicated for 10 min at room temperature, after which an almost transparent solution (with light grey tone) was formed. Furthermore, 3.9 mg of concentrated latex was distributed in 13 mL

ultrapure water. The mixture was then sonicated at room temperature for 10 min to form a uniformly distributed opaque suspension. 1 mL of the as-prepared suspension was then diluted with 9 mL of UPW and further sonicated for 10 min at room temperature.

Results and Discussion

Zeta-Potential Measurements: The ζ-potential measurments demonstrated that both the carbon black nanoparticles and concentrated latex globules had a negative surface charge in UPW. When the experiments were repeated in the ammonia solution, the surfaces of the two materials became more negatively charged. The ζ-potential results demonstrated a clear trend which is presented in Table 1.

Table 1: ζ-potential measurments of carbon black nanoparticles and concentrated latex globules in UPW and 0.01% ammonia UPW.

Material	UPW	0.01% Ammonia UPW
Carbon Black	- 38.29 ± 1.49 mV	- 63.36 ± 3.56 mV
Concentrated Latex	- 55.43 ± 2.84 mV	- 98.85 ± 2.63 mV

Latex Film Characterisation: Figure 4 shows typical AFM images of the concentrated and field latex in UPW and 0.7% ammonia UPW. The images demonstrate that the latex formed stable, mostly continuous thin films composed of globules in both of the aqueous media. This was vital for the success of the experiments as the carbon-latex interactions could only be accurately investigated if the immersed films remained adsorbed to the glass substrates with a high surface coverage. The average film thickness was measured from the AFM images using a method adopted from previous investigations.[29,30] The average film thickness for the concentrated latex was 451 ± 75 nm and 409 ± 54 nm in the UPW and 0.7% ammonia UPW, respectively. The average film thickness for the field latex was 410 ± 77 nm and 390 ± 67 nm in the UPW and 0.7% ammonia UPW, respectively. The average film thickness values are similar for the field latex and concentrated latex, which increases the consistency of the results and demonstrates that the two samples were diluted appropriately. Furthermore, the film thickness values were

also similar in the UPW and 0.7% ammonia UPW for each latex sample. Any deviations in film thickness are likely influenced by the differences in surface charge of the latex globules when immersed in the neutral UPW compared to the basic 0.7% ammonia UPW. This is because changes to the globules surface charge may have affected their packing density within the films, and consequently led to small differences in film thickness.[31,32]

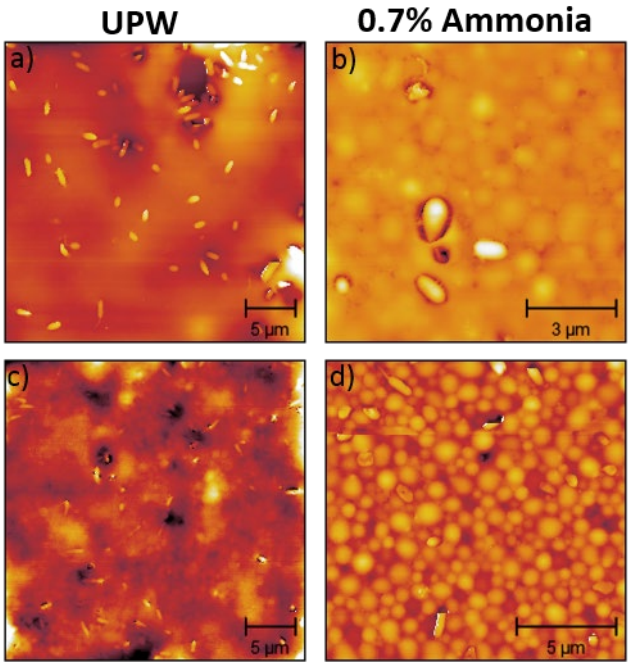

Figure 4: Typical AFM images of the latex films. a) concentrated latex in UPW, b) concentrated latex in 0.7% ammonia UPW, c) field latex in UPW, d) field latex in 0.7% ammonia UPW.

The results also demonstrated that bacteria were present in the AFM images. The bacteria appeared to protrude from the surface of the concentrated and field latex films in both UPW and 0.7% ammonia UPW. The bacteria sat on top of the latex films, significantly increasing the overall z-range of the images. Consequently, this meant that small height variations between globules were not clearly visible in the larger AFM images (Figs 4a and 4c for example). Figure 5a is a typical zoomed AFM image which clearly shows a bacterium sitting on top of the individual globules of concentrated latex in UPW. The approximate height of the protruding bacterium was 370 nm. Figure 5b is a corresponding stiffness AFM image where there is a distinct contrast between the

bacterium and the latex globules (z-range = 0 - 0.034 N/m) which confirms that they are composed of different materials. Figure 5c is a corresponding 3D image of the bacterium.

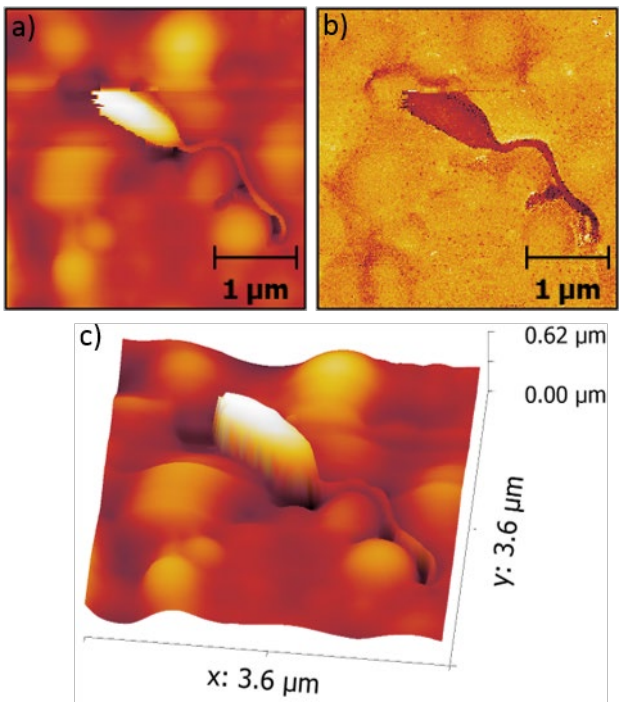

Figure 5: AFM images of a bacterium on the concentrated latex film in UPW. a) Height image, b) corresponding stiffness image, c) corresponding 3D image.

As aforementioned, natural rubber latex does not only consist of polyisoprene, it also contains a number of other components including proteins, carbohydrates and lipids.[27] Due to its varied components and harvesting methods, natural rubber latex frequently contains micro-organisms, such as bacteria.[33] The bacteria are often introduced during the maturation period, which is defined as the time in between harvesting and coagulation of the rubber.[34] Although bacteria were present on the films, the overall amount of it was very low. For instance, on the concentrated latex films, the average surface coverage of the bacteria was only 3.5 ± 0.8% and 2.9 ± 0.6% in UPW and 0.7% ammonia UPW, respectively. On the field latex films, the average surface coverage of the bacteria was also low with values of 2.9 ± 0.6% and 2.8 ± 0.7% in UPW and 0.7% ammonia UPW, respectively. Therefore, it is certain that the vast majority of the force spectroscopy

experiments took place on the latex. The results of each experiment were presented as median values from thousands of curves at many sites on the latex.

Typical Graphs: Figure 6 presents typical force-distance curves showing the carbon-concentrated latex interactions in each medium at every setpoint investigated. The graphs for the experiments in UPW fall into two distinct categories. At setpoints 0.1 nN and 0.2 nN (Figures 6a and 6c), the graphs are similar and generally repulsion is observed on the tip approach and retraction. However, at setpoints of 0.5 nN - 1.5 nN (Figures 6e, 6g and 6i), the graphs have a very different appearance as there is an initial repulsion followed by a large attraction on the tip approach and a very large adhesion on the tip retraction. This distinct difference in carbon-latex interactions in UPW at different force setpoints can be explained using DLVO theory.[35] The carbon black nanoparticles and latex globules both have a negative surface charge in UPW. Consequently, as they approach one another, electrostatic repulsion due to double-layer interactions occurs between the two materials which causes the AFM cantilever to deflect away from the latex film. Additionally, it is possible that some steric repulsion may have also contributed to the carbon-latex interactions as polymers, lipids and proteins are present on the globule surfaces.[27] If the force setpoint is larger than the magnitude of this repulsion, then the tip approach will continue and at very low separations, a strong attractive force due to short-range van der Waals interactions is experienced.[36] This attractive force overcomes the repulsion and causes the carbon-functionalised tip to jump into contact with the latex film. However, at the lower setpoints (0.1 nN and 0.2 nN), the cantilever force was generally too low to overcome the initial electrostatic/steric repulsion which meant that the tip was never brought close enough to the latex surface for significant attraction or adhesion to occur.

The typical graphs for the experiments in 0.7% ammonia UPW (Figures 6b, 6d, 6f, 6h and 6j) demonstrate that at every force setpoint, only repulsion occurred between the carbon black and concentrated latex on the tip approach. On the tip retraction, there was only significant adhesion at setpoints of 1.0 nN and 1.5 nN. Whilst Figure 6 only shows a series of typical graphs out of many thousands obtained during the experiments, it provides a good representation of the results and allows for easy visual comparisons between the style of graphs obtained at each setpoint in both aqueous media. The reason why the

carbon-latex interactions varied significantly in each medium is explained upon presentation of the full statistical analysis.

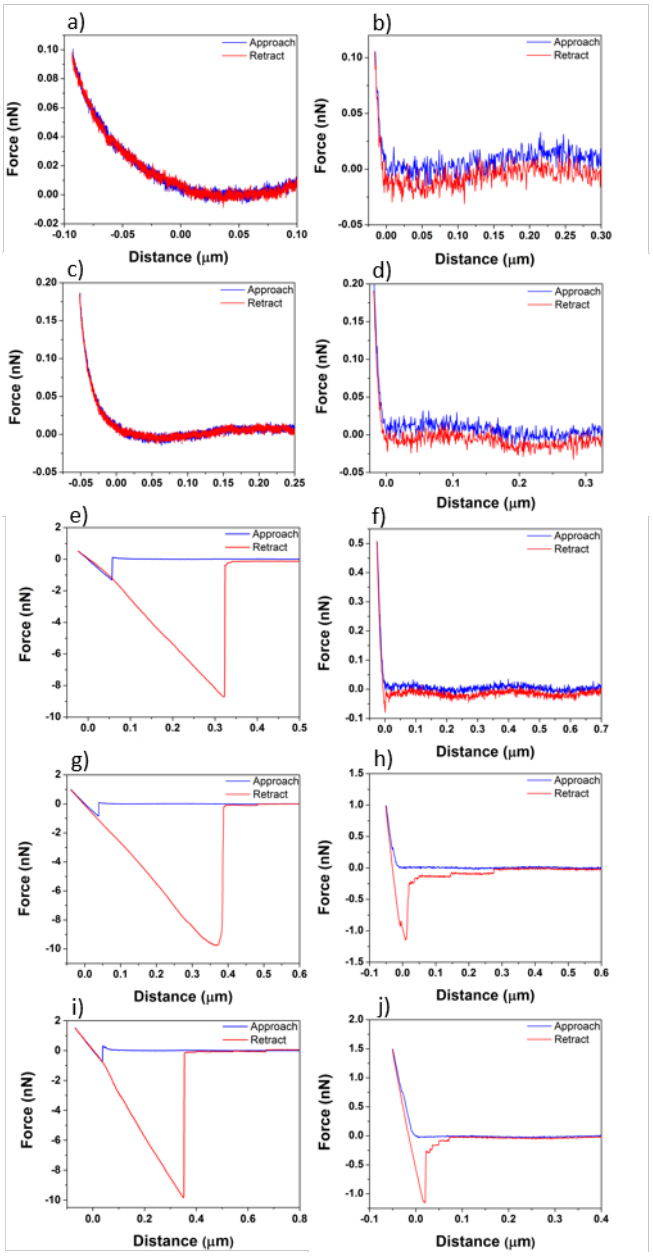

Figure 6: Typical force-distance curves showing the carbon-concentrated latex interactions in each medium at every force setpoint investigated. a) 0.1 nN in UPW, b) 0.1 nN in 0.7% ammonia UPW, c) 0.2 nN in UPW, d) 0.2 nN in 0.7% ammonia UPW, e) 0.5 nN in UPW, f) 0.5 nN in 0.7% ammonia UPW, g) 1.0 nN in UPW, h) 1.0 nN in 0.7% ammonia UPW, i) 1.5 nN in UPW, j) 1.5 nN 0.7% ammonia in UPW.

Carbon-Latex Interactions: Figure 7 presents the median attractive and adhesive force at each setpoint for the concentrated and field latex in UPW and 0.7% ammonia UPW. The maximum attractive and adhesive forces (taken as positive values) were measured from each of the force-distance curves and the following graphs were produced where the points represent the median value at each setpoint and the bars represent the maximum and minimum values within each data set. The median values with range bars were the most suitable way to present the data, as the force distributions were often skewed which meant that using average values and standard deviation bars were not appropriate.

The maximum attractive force on the tip approach and maximum adhesive force on the tip retraction provide different information regarding the carbon-latex interactions in each medium. During the tip approach, the carbon and latex were slowly moving towards one another without any contact, and consequently there are very few factors which can contribute to the attractive force. This allows the magnitude of specific forces such as van der Waals interactions to be identified. The attractive force measurements will be marginally underestimated due to the instability of the AFM cantilevers when approaching the surface. However, this does not impact our overall comparison of the interactions in each medium. Conversely, on the tip retraction, the carbon and latex are initially in contact which means that the contact area has time to develop and there are a greater number of factors which can contribute to the adhesion, such as adsorption and long-range interactions due to chain bridging. Therefore, at a given setpoint, the adhesive forces upon retraction are generally larger than the corresponding attractive force on the approach. Providing a full analysis of both attraction and adhesion is useful for many industrial processes and applications. [8,25,37]

It is important to recognise that inevitable experimental noise was present in the force-distance curves due to the AFM cantilevers being sensitive to thermal fluctuations and hydrodynamic effects.[38] This noise had a magnitude of approximately 0.02 - 0.03 nN, and therefore in curves where only repulsion was observed, the maximum attractive/adhesive force was generally measured as a value between 0.02 nN and 0.03 nN, rather than exactly 0 nN. Consequently, for any points on the graphs in Figure 7 with values of ≤0.03 nN, essentially only repulsion was observed in the force-distance curves and this small attractive/adhesive force is simply due to experimental noise.

Figure 7a shows the median attractive force for the concentrated and field latex samples in UPW. The graph demonstrates that the attractive forces were similar at each setpoint for the two different types of latex. At the setpoint of 0.1 nN, repulsion was observed for both latex samples as the cantilever force was unable to overcome the initial electrostatic/steric repulsion before withdrawing. The median attractive force then increased sharply up to the setpoint of 0.5 nN (approximate value of 0.3 nN) as the probability of the cantilever force being large enough to overcome the initial repulsion increased. At the setpoints of 0.5 nN to 1.5 nN, the cantilever force was generally large enough to overcome the initial repulsion which meant that strong attraction due to van der Waals interactions consistently occurred and led to the median values being similar to one another at the higher setpoints with an approximate value of around 0.3 nN. Figure 7c shows the median adhesive force for each latex type in UPW. The graph demonstrates that the adhesive force values were very similar for each type of latex. Furthermore, the general trend also corresponds to the attractive force graph in Figure 7a where the adhesive force rises sharply from 0.1 nN to 0.5 nN due to the increased cantilever force. It then plateaus from 0.5 nN to 1.5 nN at an approximate adhesion value of 6.5 nN. At the higher setpoints, the adhesive force in UPW is approximately an order of magnitude larger than the corresponding attractive force which was due to the additional factors as discussed previously which can contribute to the carbon-latex adhesion.

Figure 7b shows the median attractive force for each latex sample in 0.7% ammonia UPW. For the concentrated and field latex, the median attractive force values generally remain constant at each setpoint and never exceeded 0.03 nN (force of experimental noise). This demonstrates that only repulsion is generally observed on the tip approach when the experiments are performed in 0.7% ammonia UPW. Figure 7d shows the median adhesive force for each latex sample in 0.7% ammonia UPW. There is generally no adhesion for both samples at setpoints 0.1 nN and 0.2 nN. The adhesion then increases marginally for the higher setpoints (0.5 nN - 1.5 nN) and has a maximum value of 1.3 nN. The range bars on all of the graphs in Figure 7 are also generally large which was expected as many curves were obtained at different locations on the films for each setpoint, and therefore variations in the magnitude of the attractive/adhesive force was inevitable.

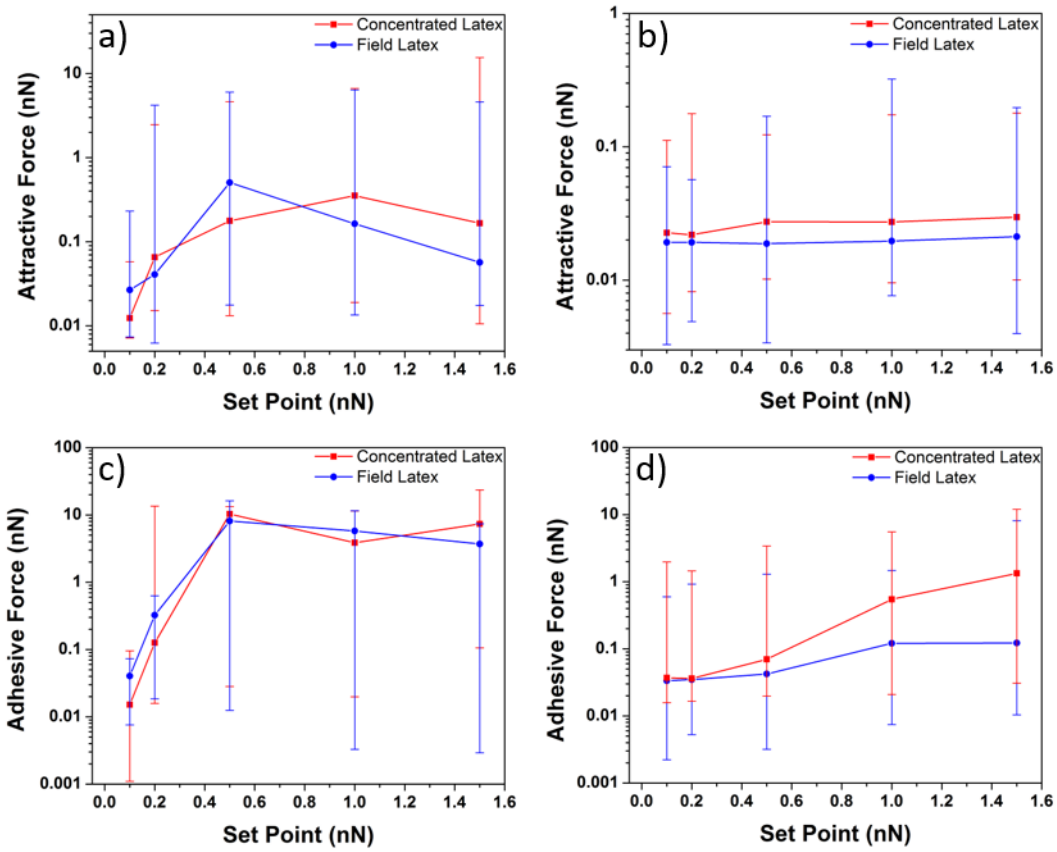

Figure 7: Graphs showing the attractive and adhesive force between the carbon and two latex samples at various force setpoints in UPW and 0.7% ammonia UPW. The points on the graphs represent the median values whilst the bars represent the overall range of the data set. a) Attractive force in UPW, b) attractive force in 0.7% ammonia UPW, c) adhesive force in UPW, d) adhesive force in 0.7% ammonia UPW.

Figure 7 demonstrates that when the experiments were carried out in UPW with a sufficiently large cantilever force, there was a significant attraction on the tip approach and a very large adhesion on the tip retraction. However, when the experiments were performed in 0.7% ammonia UPW, only repulsion occurred on the tip approach regardless of setpoint. Furthermore, on the tip retraction in 0.7% ammonia UPW, there was only adhesion at higher setpoints and it was approximately an order of magnitude smaller than the corresponding results obtained in UPW. This distinct difference in the results is because the interactions between two materials in a liquid medium are strongly influenced by the material's surface charge and also by the pH of the liquid.[31,35] The carbon black and latex globules both have negative surface charges in UPW. However, when the experiments were carried out in 0.7% ammonia UPW which has a pH of 11.6,

the surfaces became more negatively charged (confirmed with ζ-potential measurments) as the presence of ammonia attracts hydrogen ions (H^+) away from the carbon/latex surfaces.[39] This causes the electrostatic repulsion between the latex and carbon to increase significantly. Consequently, the van der Waals forces are never sufficient enough to overcome the repulsion, even at very close distances on the tip approach. Additionally, significant adhesion on the tip retraction only occurred when the setpoint was relatively high (1.0 nN - 1.5 nN). This is because the carbon black-functionalised tip was forced into firm contact with the latex globules despite the repulsive force which led to adhesive interactions. Conversely, when the experiments were performed in UPW, the surfaces had less negative surface charge as the pH of UPW is 7.0, and therefore hydrogen ions are not drawn from the surfaces. This led to some electrostatic/steric repulsion between the two negatively charged surfaces on approach. However, when the carbon-latex separation was very small, attractions due to van der Waals interactions became significant and overcame the repulsion.[36] Significant adhesion occurs on the tip retract in UPW as the carbon black-functionalised tip jumps into contact with the latex globules at setpoints of 0.5 nN - 1.5 nN which leads to strong adhesive interactions upon retraction.

It is also worth noting that the magnitude of the carbon-latex interactions were generally very similar for both the concentrated latex and field latex in each medium. These results demonstrate that even though the concentrated latex and field latex experienced different processing, it seemingly did not impact their interactions with the carbon black nanoparticles.

Conclusions

AFM force spectroscopy has been utilised to measure the interactions between carbon black nanoparticles and two types of latex in both UPW and 0.7% ammonia UPW. For the first time, carbon black nanoparticles were adhered to the AFM tips with epoxy, using force spectroscopy techniques. The tips were then thoroughly characterised using AFM imaging with a TGT1 grid and SEM imaging. Latex thin films were prepared by drop-casting onto glass substrates and were then characterised using AFM imaging in UPW and 0.7% ammonia UPW. The latex formed mostly continuous thin films composed of densely packed globules in each liquid medium. Some bacteria were present on the films which

were likely introduced during the latex's maturation period. However, the overall surface coverage of the bacteria was low, and therefore it did not impact the results significantly.

The force spectroscopy results demonstrated that the carbon-latex interactions were very different in the UPW and 0.7% ammonia UPW. For the experiments in the neutral UPW, the latex and carbon had a smaller negative surface charge which led to an initial repulsion on the tip approach. At low setpoints (0.1 nN - 0.2 nN), the cantilever force was not large enough to overcome the repulsion and the carbon black-functionalised tip never made contact with the latex. However, at higher setpoints (0.5 - 1.5 nN), the cantilever force was larger than the initial repulsion and at close tip-sample separations large attraction due to van der Waals interactions occurred. On the tip retraction in UPW, there was a very large adhesion at setpoints of 0.5 nN - 1.5 nN. Conversely, in the basic 0.7% ammonia UPW solution, hydrogen ions were drawn from the surfaces leading to significantly larger negative surface charges, and therefore only repulsion occurred between the carbon and latex on the tip approach regardless of cantilever setpoint. This change in surface charge due to the increased pH was confirmed using ζ-potential measurements. Significant adhesion only occurred at setpoints of 1.0 nN and 1.5 nN on the tip retraction and it was an order of magnitude less than the corresponding adhesion in UPW. Despite the differences in processing of the concentrated and field latex, their interactions with the carbon black nanoparticles in each medium were very similar.

The force spectroscopy investigation is the first to directly measure the interactions between carbon black nanoparticles and natural rubber latex. Consequently, the results have significance to fundamental polymer science, as well as, considerable implications within the polymer/carbon (nano)composite materials industry. In particular, the manufacture of automotive tyres where understanding the interactions between carbon black and latex within liquid media of different pH levels is vitally important in order to create high quality composites with favourable and consistent physical properties. Furthermore, we have comprehensively explained our specific experimental methodology which can be utilised to investigate many other colloidal systems.

Acknowledgments

We would like to thank Michelin for financial support on the project, as well as, providing the carbon black and latex used in the experiments. We thank Marc Couty and Matthieu Gallopin for their time, knowledge, and insightful inputs throughout the project.

Author Information

*mcclements.j@googlemail.com

*vasileios.koutsos@ed.ac.uk

Declaration of Competing Interest

The authors declare no competing financial interest.

Appendix A. Supplementary Material

AFM images of the latex thin films in air where the bacteria is embedded within the thin films. Supplementary data to this article can be found online at:

References

[1] B.N. Balzer, S. Micciulla, S. Dodoo, M. Zerball, M. Gallei, M. Rehahn, R. V Klitzing, T. Hugel, Adhesion property profiles of supported thin polymer films, ACS Appl. Mater. Interfaces. 5 (2013) 6300–6306. https://doi.org/10.1021/am4013424.

[2] J. Mcclements, V. Koutsos, Thin Polymer Film Force Spectroscopy: Single Chain Pull-out and Desorption, ACS Macro Lett. 9 (2020) 152–157. https://doi.org/10.1021/acsmacrolett.9b00894.

[3] A.M. Brzozowska, F.J. Parra-Velandia, R. Quintana, Z. Xiaoying, S.S.C. Lee, L. Chin-Sing, D. Jańczewski, S.L.M. Teo, J.G. Vancso, Biomimicking micropatterned surfaces and their effect on marine biofouling, Langmuir. 30 (2014) 9165–9175. https://doi.org/10.1021/la502006s.

[4] A.P. Duarte, J.F. Coelho, J.C. Bordado, M.T. Cidade, M.H. Gil, Surgical adhesives: Systematic review of the main types and development forecast, Prog. Polym. Sci. 37 (2012) 1031–1050. https://doi.org/10.1016/j.progpolymsci.2011.12.003.

[5] Q. Li, M. Zaiser, V. Koutsos, Carbon nanotube/epoxy resin composites using a block copolymer as a dispersing agent, Phys. Status Solidi A. 201 (2004) R89–R91. https://doi.org/10.1002/pssa.200409065.

[6] D. Mamalis, J.J. Murray, J. McClements, D. Tsikritsis, V. Koutsos, E.D. McCarthy, C.M. Ó Brádaigh, Novel carbon-fibre powder-epoxy composites: Interface phenomena and interlaminar fracture behaviour, Compos. Part B Eng. 174 (2019) 107012. https://doi.org/10.1016/j.compositesb.2019.107012.

[7] M. Bhattacharya, Polymer nanocomposites-A comparison between carbon nanotubes, graphene, and clay as nanofillers, Materials (Basel). 9 (2016) 1–35. https://doi.org/10.3390/ma9040262.

[8] M. Yang, V. Koutsos, M. Zaiser, Interactions between polymers and carbon nanotubes: A molecular dynamics study, J. Phys. Chem. B. 109 (2005) 10009–10014. https://doi.org/10.1021/jp0442403.

[9] M.I. Giannotti, G.J. Vancso, Interrogation of single synthetic polymer chains and polysaccharides by AFM-based force spectroscopy, ChemPhysChem. 8 (2007) 2290–2307. https://doi.org/10.1002/cphc.200700175.

[10] H. Haschke, M.J. Miles, V. Koutsos, Conformation of a single polyacrylamide molecule adsorbed onto a mica surface studied with atomic force microscopy, Macromolecules. 37 (2004) 3799–3803. https://doi.org/10.1021/ma035881j.

[11] M.E. McConney, S. Singamaneni, V. V. Tsukruk, Probing soft matter with the atomic force microscopies: Imaging and force spectroscopy, Polym. Rev. 50 (2010) 235–286. https://doi.org/10.1080/15583724.2010.493255.

[12] S. Kienle, M. Gallei, H. Yu, B. Zhang, S. Krysiak, B.N. Balzer, M. Rehahn, A.D. Schlüter, T. Hugel, Effect of molecular architecture on single polymer adhesion, Langmuir. 30 (2014) 4351–4357. https://doi.org/10.1021/la500783n.

[13] G. Toikka, R.A. Hayes, Direct measurement of colloidal forces between mica and silica in aqueous electrolyte, J. Colloid Interface Sci. 191 (1997) 102–109. https://doi.org/10.1006/jcis.1997.4950.

[14] S. Yasin, P.F. Luckham, Investigating the effectiveness of PEO/PPO based copolymers as dispersing agents for graphitic carbon black aqueous dispersions, Colloids Surfaces A Physicochem. Eng. Asp. 404 (2012) 25–35. https://doi.org/10.1016/j.colsurfa.2012.04.001.

[15] S. Yasin, P.F. Luckham, T. Iqbal, N. Feroz, Interaction Forces Between Graphitic Carbon Black Surfaces Coated with Polymers Using Atomic Force Microscopy, J. Dispers. Sci. Technol. 35 (2014) 1163–1168. https://doi.org/10.1080/01932691.2012.695964.

[16] J. Helenius, C.P. Heisenberg, H.E. Gaub, D.J. Muller, Single-cell force spectroscopy, J. Cell Sci. 121 (2008) 1785–1791. https://doi.org/10.1242/jcs.030999.

[17] E.J. Jamieson, C.J. Fewkes, J.D. Berry, R.R. Dagastine, Journal of Colloid and Interface Science Forces between oil drops in polymer-surfactant systems : Linking direct force measurements to microfluidic observations, J. Colloid Interface Sci. 544 (2019) 130–143. https://doi.org/10.1016/j.jcis.2019.02.051.

[18] R.F. Tabor, F. Grieser, R.R. Dagastine, D.Y.C. Chan, Measurement and analysis of forces in bubble and droplet systems using AFM, J. Colloid Interface Sci. 371 (2012) 1–14. https://doi.org/10.1016/j.jcis.2011.12.047.

[19] Q.K. Ong, I. Sokolov, Attachment of nanoparticles to the AFM tips for direct measurements of interaction between a single nanoparticle and surfaces, J. Colloid Interface Sci. 310 (2007) 385–390. https://doi.org/10.1016/j.jcis.2007.02.010.

[20] I.U. Vakarelski, S.C. Brown, B.M. Moudgil, K. Higashitani, Nanoparticle-terminated scanning probe microscopy tips and surface samples, Adv. Powder Technol. 18 (2007) 605–614. https://doi.org/10.1163/156855207782514905.

[21] X. Liu, Interactions of Silver Nanoparticles Formed in Situ on AFM Tips with Supported Lipid

Bilayers, Langmuir. 34 (2018) 10774–10781. https://doi.org/10.1021/acs.langmuir.8b01545.

[22] I.U. Vakarelski, K. Higashitani, Single-nanoparticle-terminated tips for scanning probe microscopy, Langmuir. 22 (2006) 2931–2934. https://doi.org/10.1021/la0528145.

[23] Y. Zhang, S. Ge, B. Tang, T. Koga, M.H. Rafailovich, J.C. Sokolov, D.G. Peiffer, Z. Li, A.J. Dias, K.O. McElrath, M.Y. Lin, S.K. Satija, S.G. Urquhart, H. Ade, D. Nguyen, Effect of carbon black and silica fillers in elastomer blends, Macromolecules. 34 (2001) 7056–7065. https://doi.org/10.1021/ma010183p.

[24] K. Yurekli, R. Krishnamoorti, M.F. Tse, K.O. Mcelrath, A.H. Tsou, H. Wang, Structure and Dynamics of Carbon Black-Filled Elastomers, Polym. Phys. (2001) 256–275.

[25] M.C. Strus, C.I. Cano, R.B. Pipes, C. V. Nguyen, A. Raman, Interfacial energy between carbon nanotubes and polymers measured from nanoscale peel tests in the atomic force microscope, Compos. Sci. Technol. 69 (2009) 1580–1586. https://doi.org/10.1016/j.compscitech.2009.02.026.

[26] S. Stankovich, D.A. Dikin, G.H.B. Dommett, K.M. Kohlhaas, E.J. Zimney, E.A. Stach, R.D. Piner, S.T. Nguyen, R.S. Ruoff, Graphene-based composite materials, Nature. 442 (2006) 282–286. https://doi.org/10.1038/nature04969.

[27] K. Rose, A. Steinbu, MINIREVIEWS Biodegradation of Natural Rubber and Related Compounds : Recent Insights into a Hardly Understood Catabolic Capability of Microorganisms, Appl. Environ. Microbiol. 71 (2005) 2803–2812. https://doi.org/10.1128/AEM.71.6.2803.

[28] P. Kerdtongmee, C. Pumdaung, S. Danworaphong, Quantifying dry rubber content in latex solution using an ultrasonic pulse, Meas. Sci. Rev. 14 (2014) 252–256. https://doi.org/10.2478/msr-2014-0034.

[29] J. McClements, C. Buffone, M.P. Shaver, K. Sefiane, V. Koutsos, Poly(styrene-co-butadiene) random copolymer thin films and nanostructures on a mica surface: Morphology and contact angles of nanodroplets, Soft Matter. 13 (2017) 6152–6166. https://doi.org/10.1039/c7sm00994a.

[30] J. McClements, M.P. Shaver, K. Sefiane, V. Koutsos, Morphology of Poly(styrene-co-butadiene) Random Copolymer Thin Films and Nanostructures on a Graphite Surface, Langmuir. 34 (2018) 7784–7796. https://doi.org/10.1021/acs.langmuir.8b01020.

[31] P.M. Claesson, B.W. Ninham, pH-Dependent Interactions between Adsorbed Chitosan Layers, Langmuir. 8 (1992) 1406–1412. https://doi.org/10.1021/la00041a027.

[32] M. Rutland, A. Waltermo, P. Claesson, pH-Dependent Interactions of Mica Surfaces in Aqueous Dodecylammonium/Dodecylamine Solutions, Langmuir. 8 (1992) 176–183. https://doi.org/10.1021/la00037a033.

[33] M. Oa, U. Cc, O. If, I. Ee, Current Synthetic and Systems Biology Microbiological and Physicochemical Quality of Natural and Deteriorated Rubber Latexes, Curr. Synth. Syst. Biol. 5 (2017) 1–6. https://doi.org/10.4172/2332-0737.1000133.

[34] M. Salomez, M. Subileau, J. Intapun, F. Bonfils, L. Vaysse, E. Dubreucq, Micro-organisms in latex and natural rubber coagula of Hevea brasiliensis and their impact on rubber composition , structure and properties, J. Appl. Microbiol. 117 (2014) 921–929. https://doi.org/10.1111/jam.12556.

[35] E.J.W. Verwey, Theory of the stability of lyophobic colloids, J. Phys. Colloid Chem. 51 (1947)

631–636. https://doi.org/10.1021/j150453a001.

[36] A. In, On progress in forces since the DLVO theory, Adv. Colloid Interface Sci. 83 (1999) 1–17.

[37] R. Czerw, Z. Guo, P.M. Ajayan, Y.P. Sun, D.L. Carroll, Organization of Polymers onto Carbon Nanotubes: A Route to Nanoscale Assembly, Nano Lett. 1 (2001) 423–427. https://doi.org/10.1021/nl015548y.

[38] A. Maali, C. Hurth, R. Boisgard, C. Jai, T. Cohen-Bouhacina, J.P. Aime, Hydrodynamics of oscillating atomic force microscopy cantilevers in viscous fluids, J. Appl. Phys. 97 (2005) 074907. https://doi.org/10.1063/1.1873060.

[39] R.M. Pashley, DLVO and Hydration Forces between Mica Surfaces and Li+, Na+, K+, and Cs+ Electrolyte Solutions : A Correlation of Double-Layer and Hydration Forces with Surface Cation Exchange Properties, J. Colloid Interface Sci. 83 (1981) 531–546.

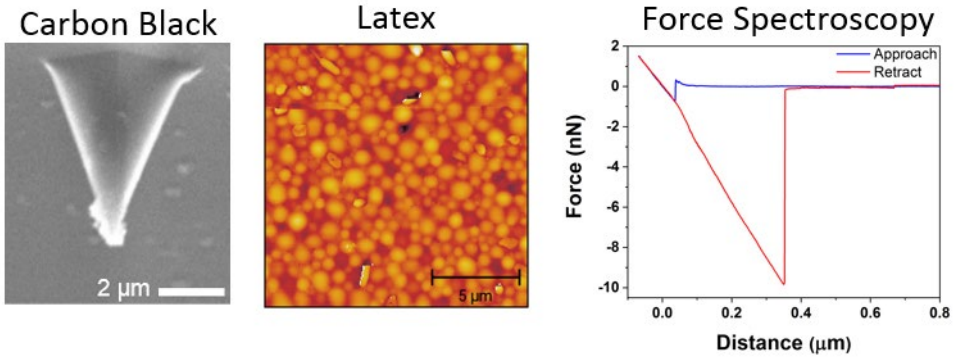

For TOC use only